

Dynamic Jet Formation from Mitigation Materials

C. Parrish and I. Worland

1 Introduction

This work has been carried out to improve the methodology and understanding of mitigating against the effects of large explosive charges. This research specifically focuses on the physical processes involved in the expansion of granular materials. This is an area which has been investigated empirically in the past [1], but still lacks a thorough understanding. Hydrocode calculations are unable to predict the inhomogeneous expansion seen in experiments [2] and thus little confidence can be held in their ability to accurately predict the mitigating mechanisms.

The regime of most interest to AWE is that of a mitigated charge in an enclosed environment where the near field effects are still prominent [3]. Prior experimental work has shown that dynamically fragmented material produces agglomerates with dimensions that are different to that of the original particulate material [4]. It is believed that the formation of these agglomerates, which at later times present themselves as jets, occurs early in the expansion of the mitigant. The use of radiography to image the early time behaviour without shrouding from the detonation products inspired a series of trials to be performed at AWE to support the early results and EDEN (Fluid Gravity Engineering) models. 1D studies in isolation showed a deceleration of a two fluid interface, indicating that Rayleigh Taylor instability [4] is a possible mechanism for formation of the initial fragments. 2D calculations using the EDEN hydrocode, when compared to experimental data suggests that Rayleigh-Taylor instability occurs on too long a timescale and does not lead to the observed jetting structure. Initial analysis of this early phase has also been undertaken by Fluid Gravity Engineering, progressing Grady [5] dynamic fragmentation theories, however, initial observations suggested that a large surface energy would be required to represent the experimental data and it is difficult to imagine such a large surface tension to be present in finer particulates such as sand.

C. Parrish · I. Worland
AWE, Aldermaston, RG7 4PR

Important observations from experiments using embedded metallic particle explosives [6] indicate that the fireball size is not related to the initial metal particle size in experiments where the mass is conserved but the particle sizes differ. Recently published work has focussed on the formation of the initial agglomerates; Frost *et al* performed a series of experiments to investigate the development of surface perturbations on packed beds during explosive events [7]. This work examines the relationship between the number of jets formed and the surface instability, referred to as the particle compaction Reynolds number. This extends the earlier work of Grady and assumes that the ratio of inertial to viscous forces acting on the particles is responsible for the granular bed breakup. This paper will consider this relationship and assess whether the AWE data contributes to this theory.

2 Experimental Evidence

An initial series of nine Rapid Prototype Design (RPD) experiments were performed at AWE in 2008 [2]. Analysis of the data from the initial trials has shown a trend between agglomerate size at break-up for the different mitigants. There is also consistency between the number of early features and late time jets. This paper details the results of four further Dynamic Fragmentation Physics (DFPhys) trials performed in 2010 to investigate system scaling. Previous mitigation trials at AWE have suggested that the mass of the system is key to the overall blast reduction [3] and so understanding if the mechanisms which are responsible for the expansion phenomenon scale with mass is of great interest.

As the previous series confirmed continuity of jet number between early and late times, the radiographic diagnostic was not required for these trials. High speed video (130,000 fps) and blast diagnostics were used to record the expansion. For simplicity of calculation a spherical geometry was used. The experimental shells were 2mm thick plastic spheres with a central spherical component for the explosive and a channel for the detonator as shown in Fig. 1. For reference see Table 1 which lists the four trial configurations.

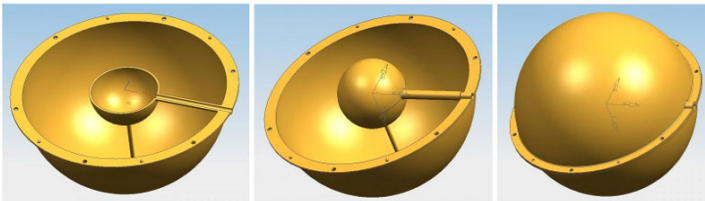


Fig. 1 DFPhys trials mitigated charge setup

Qualitative analysis of the video footage shows visible differences between the three materials as seen in Fig. 2. The two sand trials behaved as the previous RPD video footage, with distinct regular formations becoming visible soon after detonation and continuing to late times. The water displayed similar behaviour with an

Table 1 RPD and DFPhys trial configurations

| Trial | Mitigant Type | Charge Mass | Mitigant Mass | Diagnostic |
|-------|-----------------|-------------|---------------|------------------|
| DFP01 | Water | 100g | 1471g | High speed video |
| DFP02 | Dry vermiculite | 100g | 1283g | High speed video |
| DFP03 | Dry sand | 100g | 3086g | High speed video |
| DFP04 | Dry sand | 250g | 3529g | High speed video |

apparent higher frequency of structures formed. The dry vermiculite takes much longer to fragment through the shell, presumably due to the snow-plough compression process occurring due to the materials low density granular structure. Once the shell has fragmented the vermiculite expands in a similar way to the sand with more diffuse structures and an apparent fewer number. Solid fragments of the nylon shell are visible ahead of the vermiculite to late times, contrary to the water and sand videos where evidence of the shell disappears very early in the expansion. This suggests the energy available to fragment the shell is reduced by the vermiculite more effectively than the denser mitigants.

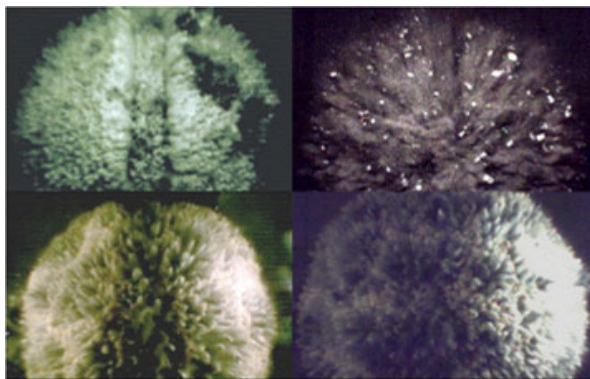


Fig. 2 Video stills from DFPhys Trials Clockwise from top left - DFPhys01 Water, DFPhys02 Vermiculite, DFPhys04 Sand, DFPhys03 Sand

Still frames from the videos were taken at suitable time intervals to provide at least four images showing clear, countable jets per trial. Having obtained the number of jets formed per experiment, the fragment size at breakup was calculated by assuming that all the mass of the experiment forms a single accretion layer as described previously [2]. This analysis, when using the predicted accretion layer density from calculations, also provides a radius of breakup for comparison. Table 2 shows a summary of the results and analysis from the trials, including the previous results from the earlier RPD series for comparison.

Table 2 RPD and DFPhys fragment breakup analysis

| Trial | Number of jets/structures | Accretion layer density kg/m^3 | Fragment radius r_f mm | Radius of break-up mm |
|------------------|---------------------------|----------------------------------|----------------------------|-------------------------|
| RPD1 Vermiculite | 378 ± 30 | 1130 | 9.22 ± 0.3 | 81.5 ± 1.3 |
| RPD2 Sand | 342 ± 40 | 1820 | 8.92 ± 0.35 | 75.0 ± 1.5 |
| RPD3 Vermiculite | n/a | n/a | n/a | n/a |
| RPD4 Sand | 365 ± 20 | 1820 | 8.72 ± 0.2 | 75.8 ± 0.8 |
| RPD5 Case | n/a | n/a | n/a | n/a |
| RPD6 Vermiculite | 450 ± 110 | 1130 | 8.38 ± 0.6 | 80.8 ± 3.0 |
| RPD7 Sand | 353 ± 40 | 1630 | 8.82 ± 0.3 | 75.4 ± 1.3 |
| RPD8 Vermiculite | 240 ± 40 | 2500 | 8.88 ± 0.4 | 62.97 ± 3.0 |
| DFPhys01 | 729 ± 289 | 1000 | 7.84 ± 0.3 | 96.2 ± 1.8 |
| DFPhys02 | 181 ± 25 | 2500 | 8.78 ± 0.25 | 53.7 ± 3.2 |
| DFPhys03 | 546 ± 110 | 1820 | 9.05 ± 0.25 | 96.2 ± 2.0 |
| DFPhys04 | 708 ± 94 | 1820 | 8.68 ± 0.3 | 105.0 ± 1.3 |

These results indicate that the trend seen in the earlier RPD experiments is not dependant on mass, as the fragment radii calculated for these trials at accretion layer density are consistent with the previous data, even after varying the system masses. This data supports the theory that the individual particles start life at approximately the same volume, however the assumption that they begin life as cubes or spheres is flawed as the radii representative of shells which would produce such particles are often smaller than the initial radius for compressible materials.

This information also suggests that the cohesion of the particles is a physical function independent of the mass of the system or material type. This implies that the theory set out by Grady [5] and developed recently by Frost *etal* [7] may explain the formation of these jets. Frost *etal* calculated the particle compaction Reynolds number for their trials and displayed it as a function of the number of jets produced for different materials. The particle compaction Reynolds number is defined below (1) where ρ is the density, U is the velocity, L is the mitigant thickness, γ_s is the particle mass density, c_s is the sound speed in the particle phase and d_s is the mean particle diameter.

$$Re = (\rho UL)/(\gamma_s c_s d_s) \quad (1)$$

The Reynolds number was calculated for all the RPD and DFPhys trials and can be seen plotted as a function of jet number in Fig. 3. The data presented here correlates well with the findings of Frost *etal*. There is a positive trend between the two variables with specific materials appearing in discreet groups. This confirms that for specific materials, the balance between the forces tending to fracture, and those tending to infinitely stretch, is proportional to the number of structures produced.

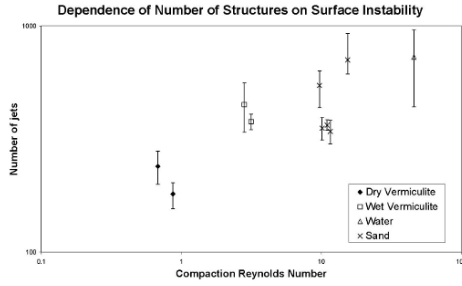


Fig. 3 Dependence of jet number on compaction Reynolds number

3 Calculations

One-dimensional calculations of the four DFPhys trials were performed in EDEN utilising the two-phase model and a cell size no greater than 0.2 mm. The best way to display such calculations is in the form of a density map as in Fig. 4. The greyscale on the plots represents the density of the mitigation, with the shock and detonation products overlaid in red and green. Also plotted is the experiment outer mitigation radius as obtained from the high speed videos, as blue crosses. This outer radius is not expected to represent the position of the accretion layer but either the outer case or detonation products as these can both shroud the accretion layer from view.

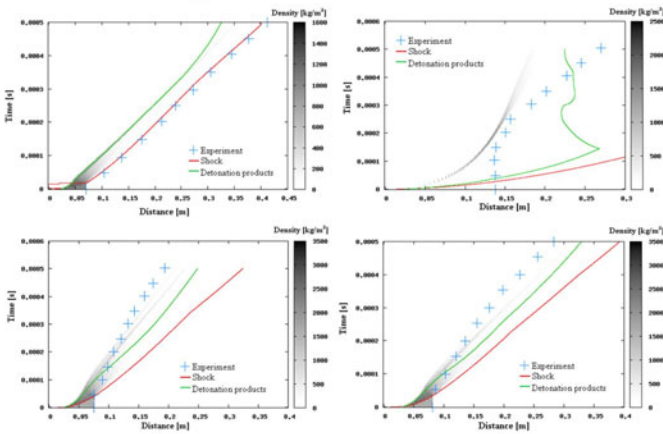


Fig. 4 Density profile maps Clockwise from top left - DFPhys01 Water, DFPhys02 Vermiculite, DFPhys04 Sand, DFPhys03 Sand

It can be seen that the calculation of DFPhys01 is a good representation of the experiment as the outer radius in the videos closely follows the outer spill layer in the simulation with the correct expansion velocity. The agreement is much less close with the remaining trials. The experimental expansion for DFPhys02 was difficult to determine from the videos as the material was so diffuse and the detonation products obscured the mitigant for most of the early stages. As a result the comparison to the 1D simulation shows the experimental velocity to be much higher than the calculated one, although not as fast as the detonation products. It is likely that a combination of the detonation products and the mitigation are observed and that distinguishing between the two as the detonation products become more diffuse is unachievable.

Both DFPhys03 and 04 behave in very similar ways, which is reassuring for both the simulations and the experimental results. In both cases the calculations predict that the sand will expand with a higher velocity than is observed on the experiments. The video images were clear and there was very little shrouding from detonation products at later times. Despite this the observed velocity was still less than that predicted. As the simulation does not represent the formation of jets or structures it could be attributed to the drag force discrepancy between individual particles as calculated in EDEN, or larger clumps of particles as visible in the experiment.

When considering the peak overpressure and impulse for each trial, a comparison has been made between those points where the side-on pressure was measured and those measuring the reflected pressure. The code to experiment comparisons are shown in Fig. 5. It can be seen that the side-on pressure is better represented by the 1D calculation than the reflected pressure. These plots also show that the calculations slightly under predict the peak pressure and over predict the impulse for the reflected pressure measurements. This indicates that the reflected pressure gauges may not be recording the incidence of the mitigating material properly. Additionally, the 1D calculations do not take into account reflections from surrounding objects which may amplify the peak overpressure. Further 2D calculations may improve the peak pressure predictions in this case.

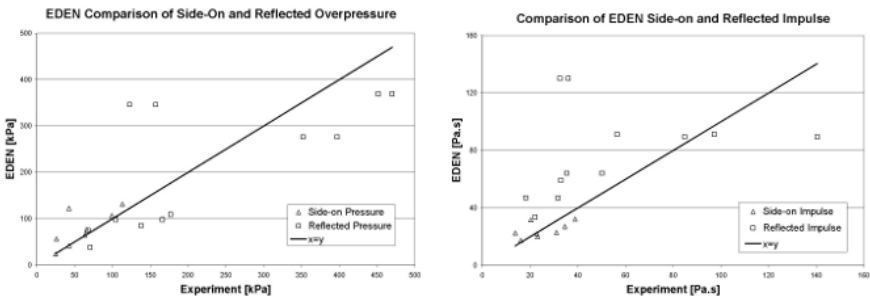


Fig. 5 Comparison of calculation and experiment for blast parameters

4 Conclusions and Discussion

The aim of this work was to investigate the mechanisms responsible for the inhomogeneous expansion of granular materials with the goal of more accurate computational representation. Analysis of the data shows similarities in the structure formation volumes for the different mitigant types, regardless of system masses. This suggests an inherent property of the process rather than the system variables. Comparison of the results to a theory building on the work of Grady [7] suggests that the structures may be the result of the ratio of inertial to viscous forces on the compacted layer of material. While an abundance of inertial forces would represent a situation where the bed fractured dispersedly; a dominance in viscous forces would suggest an infinitely expanding, thinning shell. The ratio of these forces should therefore be proportional to the number of structures formed for a given material irrespective of the system scale; this is evident in the graphical representation of these trials.

Comparison of the experimental velocity data to the EDEN hydrocode highlights the need for accurate equation of state data for the more complex materials. One-dimensional calculations of the incident blast pressure and impulse for the well characterised materials gave good results, suggesting the inhomogeneous expansion does not greatly affect these blast parameters. The data also showed that when considering additional complexities as reflections from boundaries and objects, one dimension is not a sufficient representation.

References

1. Zhang, F., Frost, D.L., et al.: Explosive Dispersal of Solid Particles. *Shock Waves* 10, 431–443 (2001)
2. Milne, A.M., Parrish, C.E., Worland, I.: Dynamic fragmentation of Blast Mitigants. *Shock Waves* 20, 41–51 (2010)
3. Parrish, C.E., Worland, I.: Numerical modelling of blast mitigation systems. In: Proceedings of 21st International Symposium on Military Aspects of Blast and Shock, Israel, October 4–8 (2010)
4. Youngs, D.L.: Numerical simulation of mixing by Rayleigh-Taylor and Richtmyer-Meshkov instabilities. *Laser Particle Beams* 12, 725–750 (1994)
5. Grady, D.E.: Local inertial effects in dynamic fragmentation. *J. Appl. Phys.* 53, 322–325 (1982)
6. Ritzel, D.V., Ripley, R.C., Murray, S.B., Anderson, J.: Near field blast phenomenology of thermobaric explosions. In: Proceedings of the 26th International Symposium on Shock Waves, Gttingen, vol. 1, pp. 305–310 (2007)
7. Frost, D.L.: Jet Formation During Explosive Particle Dispersal. In: Proceedings of 21st International Symposium on Military Aspects of Blast and Shock (2010)